TECHNICAL MEMORANDUMS

NATIONAL ADVISORY COMMITTEE FOR AERONAUTICS

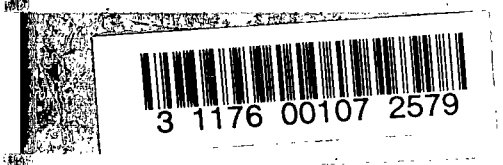

No. 1003

THE RESISTANCE COEFFICIENT OF COMMERCIAL ROUND WIRE GRIDS

By B. Eckert and F. Pflüger

Luftfahrtforschung
Vol. 18, no. 4, April 22, 1941
Verlag von R. Oldenbourg, München und Berlin

Washington
January 1942

NATIONAL ADVISORY COMMITTEE FOR AERONAUTICS

TECHNICAL MEMORANDUM NO. 1003

THE RESISTANCE COEFFICIENT OF COMMERCIAL ROUND WIRE GRIDS*

By B. Eckert and F. Pflüger

SUMMARY

The resistance coefficients of commercial types of round wire grids were examined for the purpose of obtaining the necessary data on supercharger test stands for throttling the inducted air to a pressure corresponding to a desired air density. The measurements of the coefficients ranged up to Reynolds numbers of 1000. In the arrangement of two grids in tandem, which was necessary in order to obtain high resistance coefficients, the relationship of the coefficients with the solidity, that is, mesh density of grid, was found to be accompanied by a further relationship with the mutual spacing of the individual grids.

Notation

N performance (mkg/s)

G weight of air consumed per second (kg/s)

V volume of air consumed per second (m^3/s)

V_H displacement of engine (m^3)

H delivery head (m)

n revolutions per minute

a operating cycles per revolution

λ excess air factor

γ specific weight of air (kg/m^3)

ρ air density (kg^2/m^4)

---

*"Bestimmung der Widerstandsbeiwerte handelsüblicher Rundrahtsiebe." Luftfahrtforschung, vol. 18, no. 4, April 22, 1941, pp. 142-46.

f rate of flow

v rate of flow of air through section (m/s)

p_{St_1} static pressure at entry (mm WS)

p_{St_2} static pressure upstream from grid (mm WS)

p_{St_3} static pressure downstream from grid (mm WS)

$\Delta p = \Delta_v p$ pressure drop across the grid (mm WS)

Δp_{id} pressure drop by potential flow (mm WS)

W air resistance (kg)

c_w resistance coefficient

$F = F_2$ test section and area of grid boundary (m^2)

F_R projected area of grid (m^2)

$F_1 = F - F_R$ free section of grid (m^2)

$\varphi = \frac{F_R}{F}$ solidity

S wire gage

z mesh per centimeter

Re Reynolds number

υ kinematic viscosity (m^2/s)

INTRODUCTION

The power of an airplane supercharger decreases with increasing operating height by equal air volume (m^3/s) — referred to induction state — as a result of the decreasing air density. So, unless special provisions are made for the study of such superchargers on test stands not operating under altitude conditions, much greater power is required than for the same supercharger at the proposed operating level, because the density of the inducted air at sea level is greater.

The supercharger power required ordinarily amounts to

$$N_{supercharger} = \frac{G\ H}{\eta} = \frac{V\ \gamma\ H}{\eta} \quad \left[\frac{mkg}{s}\right] \tag{1}$$

the air volume V being given by

$$V = \frac{n}{a}\ V_H\ \lambda\ \eta_v \quad \left[\frac{m^3}{s}\right]$$

where η_v is volumetric efficiency; V is therefore independent of the operating height.

To illustrate: If a supercharger designed for 8 kilometers critical altitude is tested under sea-level conditions (1.033 kg/cm^2 and t = 15° C, point A in fig. 1), the supercharger power required amounts to

$$N_{o\ km} = \frac{V\ H}{\eta}\ 1.226 \quad \left[\frac{mkg}{s}\right]$$

as compared to

$$N_{8\ km} = \frac{V\ H}{\eta}\ 0.525 \quad \left[\frac{mkg}{s}\right]$$

required at 8 kilometers altitude (point B, fig. 1). By equal delivery head, therefore, the increase in power required at sea level is:

$$\frac{N_{o\ km} - N_{8\ km}}{N_{8\ km}} = \frac{1.226}{0.525} - 1 = 2.34 - 1 = 1.34$$

These increases in supercharger power can be avoided in sea-level operating tests by throttling, that is, by lowering the pressure of the induction air. Since throttling processes are practically isothermic, a grid, for instance, before the supercharger entrance opening produces an air density corresponding to the critical altitude. Applied to the foregoing example, the power (point C, fig. 1) then amounts to

$$N_{o\ throttled} = \frac{V\ H}{\eta}\ 0.525 \quad \left[\frac{mkg}{s}\right]$$

A pressure drop across the grid from D to C (fig. 1) is thereby achieved. With c_w as the resistance coefficient of the throttle, the pressure drop is

$$\Delta p = \frac{\rho}{2} v^2 c_w \qquad (2)$$

Superficial investigations indicated that the air density ρ prevailing behind the throttling point would be practible in equation (2). Applied to the example shown in figure 1, the air density given for point C should then be used as a basis for the solution.

The simplest throttling means are wire grids.

EXPERIMENTAL PROCEDURE

The resistance coefficients of the different round wire grids were determined in a supercharger test stand of the Stuttgart Research Institute, admittedly at such low air speed that the density variations relative to the experimental evaluation could be disregarded. The experimental set-up along with the test stations is shown in figure 2.

An axial blower sucks the air through the entrance cone; the grids of varying solidities mounted between two flanges were tested between entrance cone and blower. The air leaves the test section by way of a fine throttling device (Prasil type) which was kept wide open during the resistance measurements. By varying the engine speed the air speed could be increased to 30 meters per second.

To determine the air speed the static pressure was recorded at the entry (test station 1, fig. 2); while the recording of the pressure upstream (test station 2) and downstream (station 3) from the grid afforded the pressure drop across the grid. Betz micromanometers were used.

TEST GRIDS

The experiments extended to commercial round wire grids with square mesh. The wire gage of all grids was the same, except one, grid no. XVI, which disclosed two different gages in its texture.

Wire gage and mesh were measured very carefully and the solidity of the separate grids defined accordingly. In some tests the number of grids was doubled; in others different grids were arranged in tandem and their resistance coefficients defined. Table 1 contains a list of the explored grids and grid combinations with their characteristic data.

On two grids a and b arranged in tandem the mean wire gage δ_m was determined at

$$\delta_m = \frac{z_a \delta_a + z_b \delta_b}{z_a + z_b} \tag{3}$$

INTERPRETATION

a) Determination of Undisturbed Inflow Velocity

The low-pressure recorded at station 1 (fig. 2) is a measure for the speed in the section. With f as a cone correction factor

$$\frac{\rho}{2} v^2 = f \Delta p_{St_1} \tag{4}$$

or

$$v = \sqrt{\frac{f}{\rho/2} \Delta p_{St_1}}$$

b) Determination of Resistance Coefficient

Defining

$$c_w = \frac{W}{\frac{\rho}{2} v^2 F} \tag{5}$$

as resistance coefficient of a grid and posting

$$W = (p_2 - p_3) F = \Delta p F \qquad [kg] \tag{6}$$

we get

$$c_w = \frac{\Delta p}{\frac{\rho}{2} v^2} \tag{7}$$

Δp is the pressure difference between station 2 and station 3 (fig. 2); hence the pressure loss across the grid.

Table 1.- Grids and Combinations

Number	Grid number	Mesh per centimeter	Wire gage (mm)	Solidity $\varphi = \frac{F_R}{F}$
1	I	1.5	0.7	0.212
2	II	2.2	.6	.265
3	III	3.0	.45	.252
4	IV	4.6	.3	.257
5	V	7.2	.25	.328
6	VI	9.5	.25	.419
7	VII	14.5	.2	.496
8	VIII	18.5	.16	.505
9	IX	22.5	.14	.53
10	X	25.5	.14	.587
11	XI	28.0	.12	.559
12	XII	29.0	.17	.743
13	XIII	31.5	.15	.723
14	XIV	34.0	.1	.564
15	XV	37.0	.1	.603
16	XVI	42.0	.26	.957
17	XIII + V	38.7	.17	.882
18	XII + VI	38.5	.19	.92
19	XII + VII	43.5	.18	.951
20	XII + VIII	47.5	.166	.955
21	XII + IX	57.0	.1455	.962
22	XII + XV	66.0	.131	.982
23	2 × XIII	63.0	.15	.997

c) Definition of Projected Area of Grid and Solidity

With F_R as projected area of wire exposed to air stream and F as area of grid boundary, the solidity (reference 1) is:

$$\varphi = \frac{F_R}{F} \tag{8}$$

hence φ is a measure for the grid density. The total projected area of the grid follows as the sum of the projections of all wires. Referred to unit area ΔF (10 mm × 10 mm = 100 mm²) the projected area for z wires of 10 mm each and a wire gage δ is:

$$\Delta F_R = 10\, z\delta + 10\, z\delta - (z\delta)^2$$

$$\Delta F_R = 20\, z\delta - (z\delta)^2 = z\delta(20 - z\delta) \qquad [mm^2] \qquad (9)$$

hence the solidity:

$$\varphi = \frac{\Delta F_R}{\Delta F} = \frac{z\delta\,(20 - z\delta)}{100} \qquad (8)$$

The minor discrepancies at the pipe circumference can be disregarded.

RESULTS OF TESTS

Figure 3 shows the resistance coefficient c_w of the round wire grids listed in table 1 plotted against the undisturbed flow velocity.

The resistance coefficients of several grids with small solidity as obtained by measurement are presented in figure 4; whereas in figure 5 the resistance coefficients are plotted against the Reynolds number Re, where

$$Re = \frac{\delta\, v}{\nu} \qquad (10)$$

Corresponding to the mean test condition, the kinematic viscosity was based on 750 millimeters mercury and 20° C, that is

$$\nu = 14 \times 10^{-6}\ m^2/s$$

An increase in air speed, that is, increase in Reynolds number is accompanied by a drop in resistance coefficient. The thin cylindrical wires of which the grids are manufactured, disclose a relationship with the Reynolds number similar to the cylinder tests in wind tunnels. Because of the well-rounded bell mouth and the short distance of the grid away from it the inflow is largely laminar. An increase in air speed, that is, a

resistance measurement at Reynolds numbers of $Re > 1000$ was experimentally impossible.

The experiments with double grids showed that, when arranged close together without intermediate space, the total resistance coefficient is lower than the sum of the two separate resistance coefficients. This phenomenon is attributable to the fact that the solidity of the two grids is unable to become fully effective, that is, some wire overlap exists - even if only partial. On very narrow-mesh grids the mutual spacing is of less importance for the total resistance coefficient. The total resistance coefficients of two grids spaced 10 millimeters apart approximately equals the sum of the separate resistance coefficients.

Figure 6 shows the resistance coefficients c_w of the explored grids plotted against the solidity φ at $Re = 200$. From the data provided, it is easy to compute the necessary solidity φ for a desired c_w or the number of meshes z for a given wire gage δ.

Example: Suppose the necessary resistance coefficient c_w for the required throttling is 13.

Figure 6 gives for $Re = 200$ and $c_w = 13$ a solidity φ of 0.78. With a reference area $\Delta F = 100$ square millimeters, the necessary projected area ΔF_R of the wires is

$$\Delta F_R = \varphi \Delta F = 78 \text{ mm}^2$$

The mesh required for a wire gage $\delta = 0.1$ can be computed from $0.78 = z\ 0.1(2 - z\ 0.1)$, that is: $Z = 53$ mesh per centimeter.

THEORETICAL RESISTANCE COEFFICIENT OF A GRID

With the identification of figure 7 the continuity equation reads:

$$\rho_0 F_0 v_0 = \rho_1 F_1 v_1 = \rho_2 F_2 v_2 \qquad (11)$$

Suppose that

$$F_0 = F_2; \quad \rho_0 = \rho_1 = \rho_2 = \rho \qquad (12)$$

Then, for potential flow, the pressure equation would give

$$p_{o\,(id)} + \frac{\rho}{2} v_o^2 = p_{1\,id} + \frac{\rho}{2} v_1^2 = p_{2\,id} + \frac{\rho}{2} v_2^2 \qquad (13)$$

Upstream from the grid the flow can be summarily dealt with as free from loss; thus the actual pressure becomes

$$p_o = p_{o\,id} \quad \text{and} \quad p_1 = p_{1\,id}$$

Downstream from the grid the flow is not free from losses, since it separates in vicinity of the narrowest cross section. Behind the wires of the grid a dead air region develops, which in the further course of the flow is, however, equalized again by mixing, so that the speed in flow section F_2 may be treated again as uniformly distributed. But the pressure in section F_2 is smaller by a pressure loss $\Delta_v p$ than pressure $p_{2\,id}$ in loss-free flow, that is,

$$p_2 = p_{2\,id} - \Delta_v p$$

In order that this pressure loss may be computed, it is assumed that the sum of the narrowest sections of the jets bounding the dead-air region is equal to the sum of the narrowest cross sections F_1 of the grid and that the speed along this section is uniformly distributed. The pressure on the lee side of the wires, that is, at the wire-side boundary of the dead-air region, is nearly constant and is therefore hereinafter assumed to be equal to the pressure p_1 in section F_1.

Since $F_1 + F_R = F_o$, the total stream force P_{II} acting on the boundary of zone II (fig. 7) is:

$$P_{II} = m(v_1 - v_2) + (p_1 - p_2) F_o = 0 \qquad (14)$$

where, with

$$m = \rho v_o F_o \quad \text{and} \quad v_2 = v_o$$

there follows

$$p_2 - p_1 = p_{2\,id} - p_1 - \Delta_v p = \rho v_o(v_1 - v_o) \qquad (15)$$

or with

$$p_{2\,id} - p_1 = \frac{\rho}{2} (v_1^2 - v_o^2)$$

$$\Delta_v p = \frac{\rho}{2}(v_1^2 - v_o^2) - \rho v_o(v_1 - v_o) \qquad (16)$$

$$\Delta_v p = \frac{\rho}{2} v_0^2 \left(\frac{v_1}{v_0} - 1 \right)^2 \tag{17}$$

The total stream force P_I acting along the boundary of zone I is also equal to zero. Hence the resistance W acting on the grid is equal to the product of the pressure difference $\Delta_v p$ between sections 0 and 2 and the cross-sectional areas F_0 and F_2.

$$W = \Delta_v p F_0 \tag{18}$$

For a resistance coefficient of

$$c_w = \frac{W}{\frac{\rho}{2} v_0^2 F_0} \tag{19}$$

it then affords

$$c_w = \frac{\Delta_v p}{\frac{\rho}{2} v_0^2} = \left(\frac{v_1}{v_0} - 1 \right)^2 = \left(\frac{F_2}{F_1} - 1 \right)^2 \tag{20}$$

or

$$\frac{F_2}{F_1} = \sqrt{c_w} + 1 \tag{21}$$

With the notation

$F_2 = F$ = area of grid boundary

$F_1 = F - F_R$ = free section of grid

$$c_{w\,theor} = \left(\frac{F}{F - F_R} - 1 \right)^2 = \left(\frac{F_R}{F - F_R} \right)^2 = \left(\frac{\varphi}{1 - \varphi} \right)^2 \tag{22}$$

These theoretical values of c_w are shown as dashed curve in figure 6. The agreement between theory and experiment is satisfactory, considering that the tests were made at comparatively low Reynolds numbers and that the basic assumptions are, after all, somewhat crude.

For double grids (a and b) the theoretical $c_{w\,theor}$ was determined in correspondence with the mean solidity φ_{tot} from

$$c_{w_{tot_{theor}}} = c_{w_{a_{theor}}} + c_{w_{b_{theor}}} \tag{23}$$

and

$$\left(\frac{\varphi_{tot}}{1-\varphi_{tot}}\right)^2 = \left(\frac{\varphi_a}{1-\varphi_a}\right)^2 + \left(\frac{\varphi_b}{1-\varphi_b}\right)^2 \tag{24}$$

at

$$\varphi_{tot} = \frac{\sqrt{\left(\frac{\varphi_a}{1-\varphi_a}\right)^2 + \left(\frac{\varphi_b}{1-\varphi_b}\right)^2}}{2 + \sqrt{\left(\frac{\varphi_a}{1-\varphi_a}\right)^2 + \left(\frac{\varphi_b}{1-\varphi_b}\right)^2}} \tag{25}$$

Here also agreement with experimental values is obtained, provided the solidity for grids mounted one behind the other is computed according to equation (25)

Translation by J. Vanier,
National Advisory Committee
for Aeronautics.

REFERENCE

1. Flachsbart, O.: Widerstand von Seidengazefiltern. Runddraht- und Blechstreifensieben mit quadratischen Maschen. Ergebn. Aerodyn. Versuchsanst. Göttingen, IV. Lfg., München 1932, R. Oldenbourg.

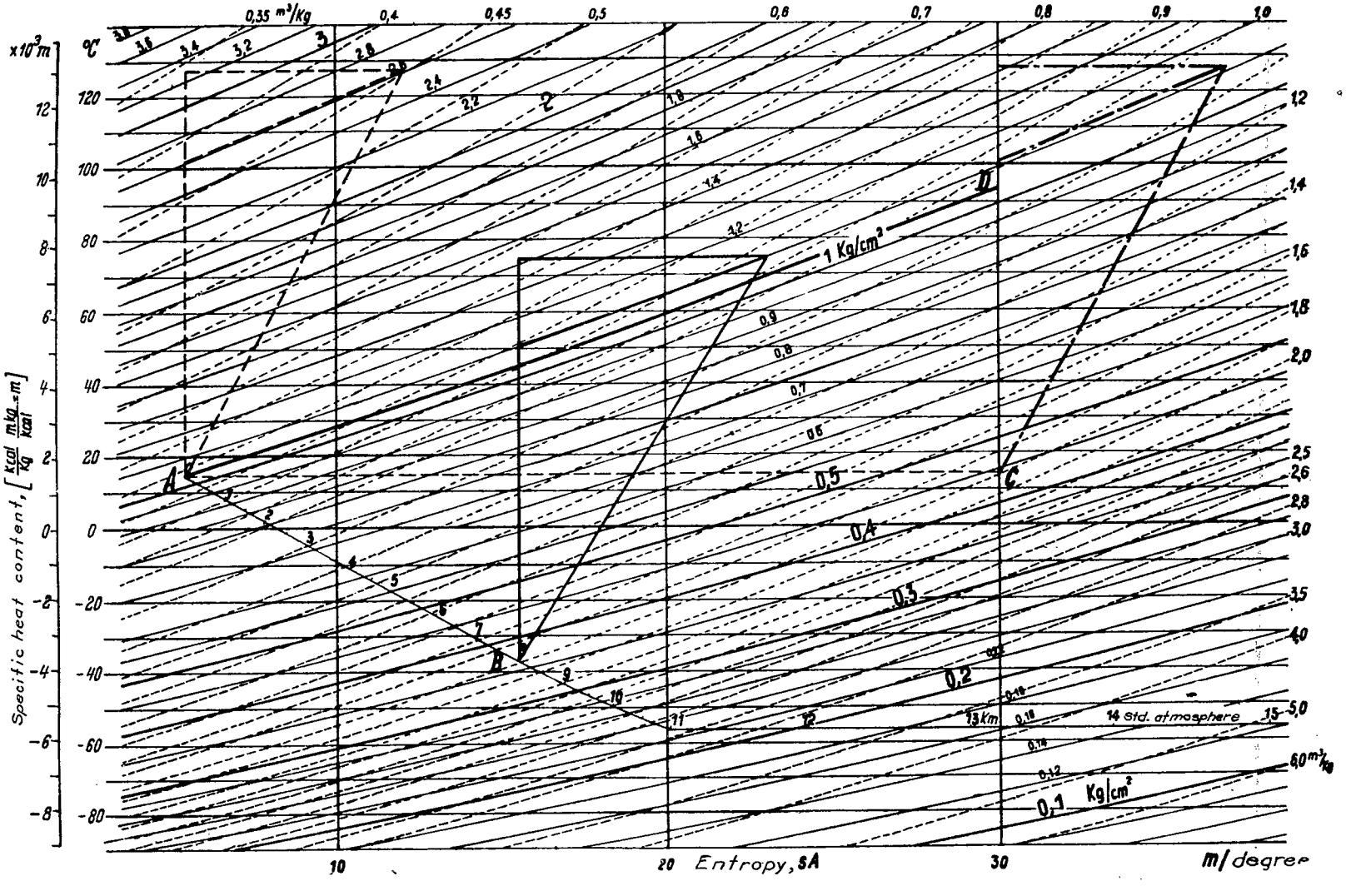

Figure 1.- I-S diagram of atmospheric air.

Fig. 1

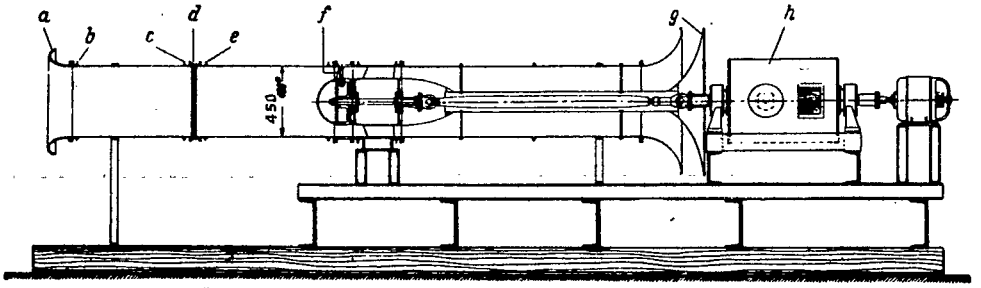

Figure 2.- Test lay-out for measuring the resistance coefficients of round-wire grids.

(a) Bell mouth. (b) Test station 1. (c) Test station 2.
(d) Grid. (e) Test station 3. (f) Axial fan.
(g) Throttling device. (h) Driving motor.

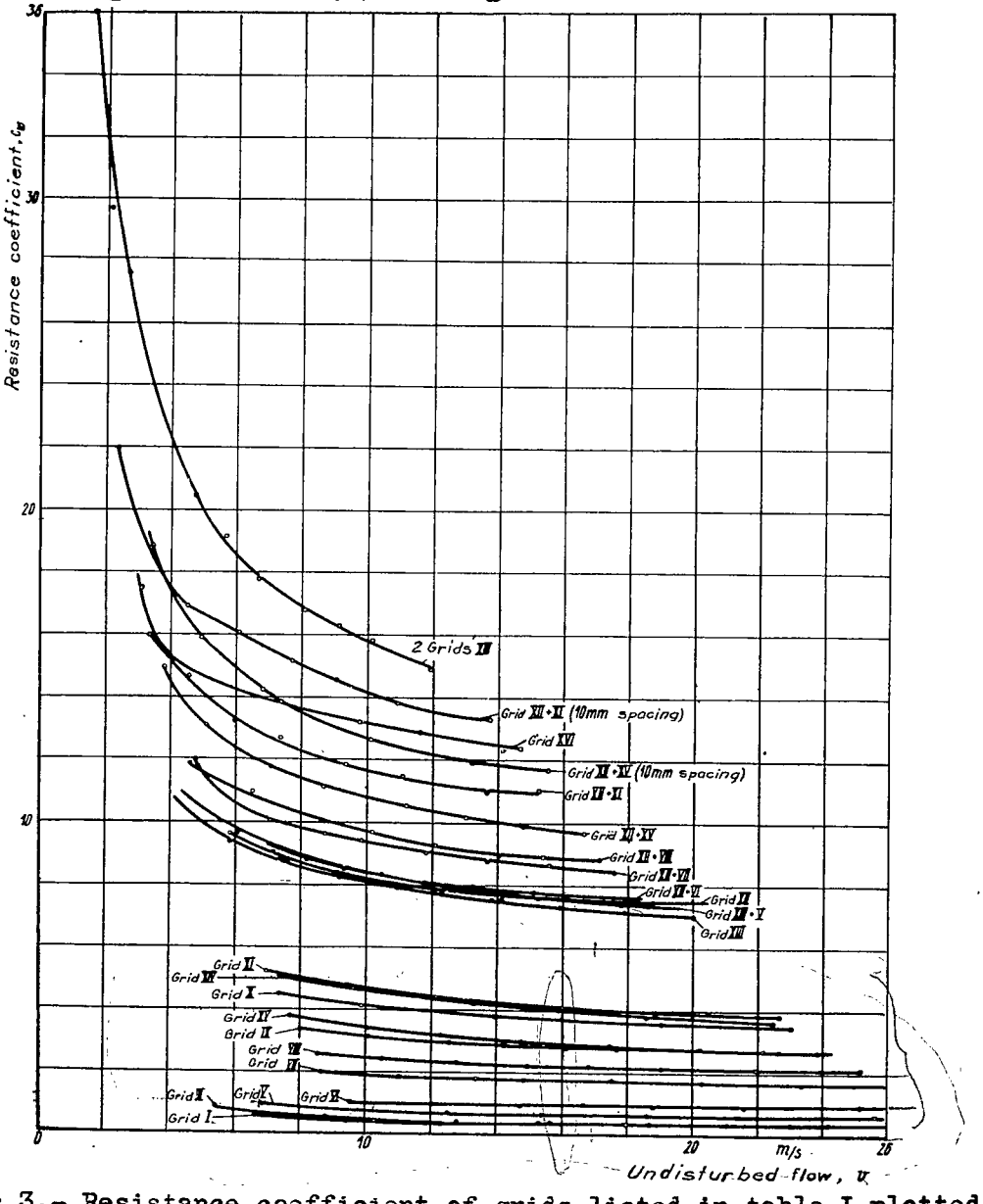

Figure 3.- Resistance coefficient of grids listed in table I plotted against undisturbed axial velocity.

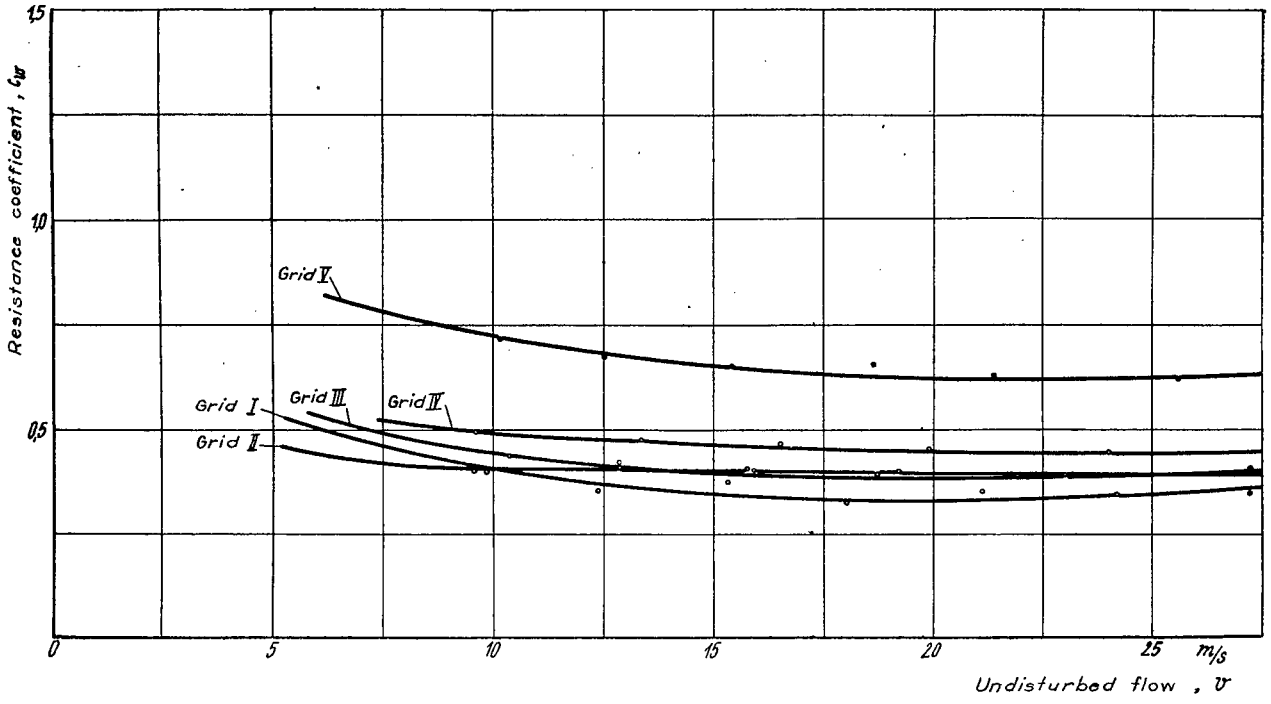

Figure 4.- Resistance coefficient of various grids with small solidity plotted against undisturbed axial velocity.

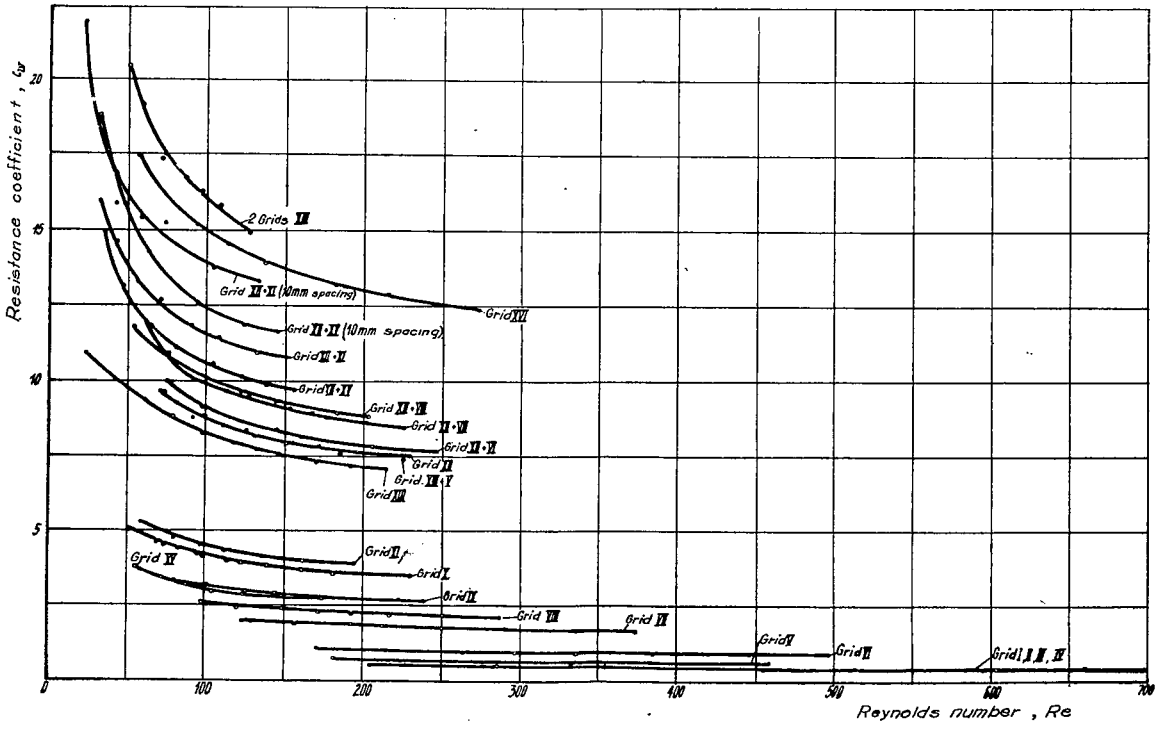

Figure 5.- Resistance coefficient of grids plotted against Reynolds number.

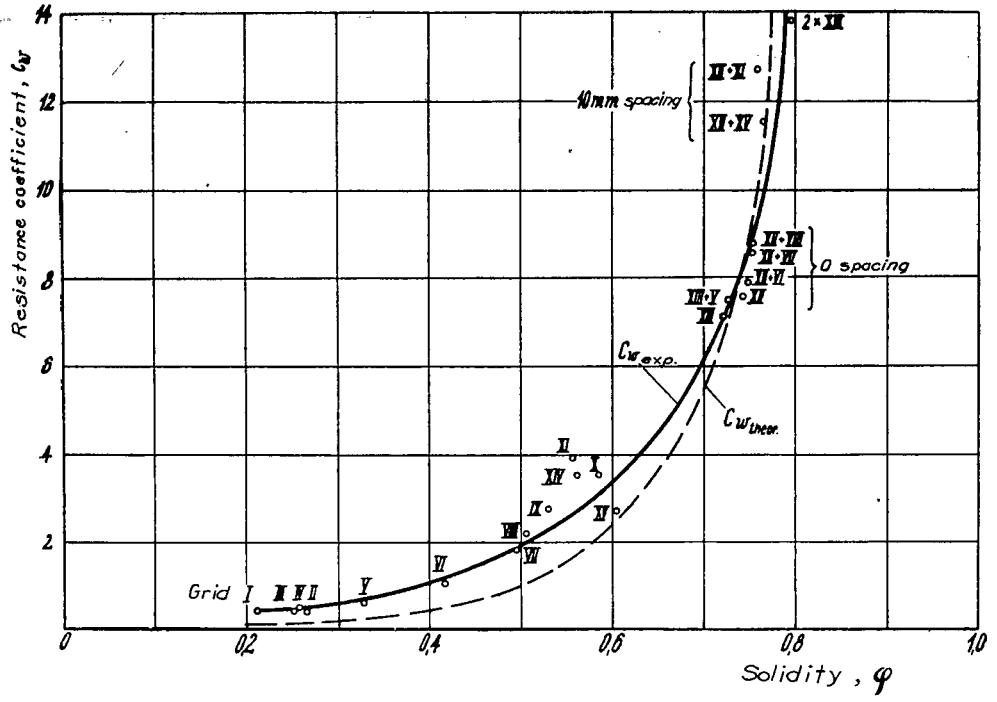

Figure 6.- Resistance coefficient of grids plotted against solidity (Re = 200).

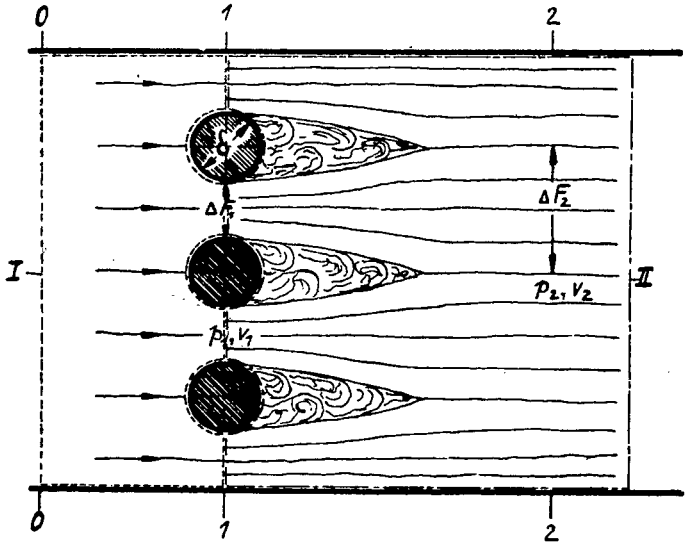

Figure 7.- Illustration of throttling process in a grid.